ACS OMEGA

ACS AUTHORCHOICE

http://pubs.acs.org/journal/acsodf

Article

Paper Thermoelectrics by a Solvent-Free Drawing Method of All Carbon-Based Materials

Saqib Rafique, Nafiseh Badiei, Matthew R. Burton,* Jorge Eduardo Gonzalez-Feijoo, Matthew J. Carnie, Afshin Tarat, and Lijie Li*

Cite This: *ACS Omega* 2021, 6, 5019−5026

Read Online

ACCESS | Metrics & More | Article Recommendations

ABSTRACT: As practical interest in the flexible or wearable thermoelectric generators (TEGs) has increased, the demand for the high-performance TEGs based on ecofriendly, mechanically resilient, and economically viable TEGs as alternatives to the brittle inorganic materials is growing. Organic or hybrid thermoelectric (TE) materials have been employed in flexible TEGs; however, their fabrication is normally carried out using wet processing such as spin-coating or screen printing. These techniques require materials dissolved or dispersed in solvents; thus, they limit the substrate choice. Herein, we have rationally designed solvent-free, all carbon-based TEGs dry-drawn on a regular office paper using few-layered graphene (FLG). This technique showed very good TE parameters, yielding a power factor of 97 μW m^{-1} K^{-2} at low temperatures. The p-type only device exhibited an output power of up to ∼19.48 nW. As a proof of concept, all carbon-based p-n TEGs were created on paper with the addition of HB pencil traces. The HB pencil exhibited low Seebeck coefficients (−7 μV K^{-1}), and the traces were highly resistive compared to FLG traces, which resulted in significantly lower output power compared to the p-type only TEG. The demonstration of all carbon-based TEGs drawn on paper highlights the potential for future low-cost, flexible, and almost instantaneously created TEGs for low-power applications.

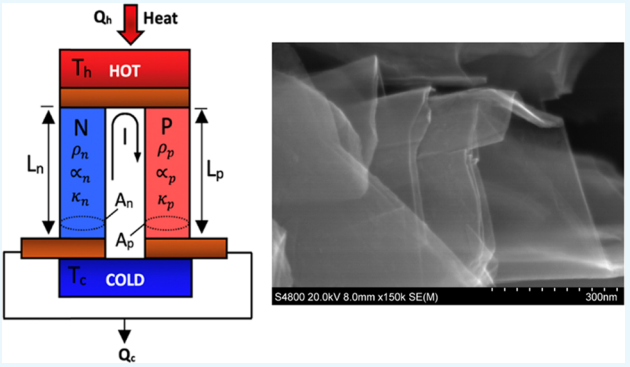

1. INTRODUCTION

Over 70% of the global primary energy is reported to dissipate as heat below 100 °C, which ultimately can lead to the environmental and resource management issues.[1] The use of this wasted heat by harvesting electrical energy could be advantageous. Thermoelectric generators (TEGs) can transform a proportion of this wasted heat energy directly into electrical energy using the Seebeck effect.[2,3] The performance of a thermoelectric (TE) material is typically evaluated by the dimensionless figure of merit ($ZT = S^2\sigma T\kappa^{-1}$), where S represents the Seebeck coefficient (V K^{-1}), σ denotes the electrical conductivity (S m^{-1}), T is the absolute temperature (K), and κ denotes the thermal conductivity (W m^{-1} K^{-1}).[4,5] The term $S^2\sigma$ is known as the power factor (W m^{-1} K^{-2}) and correlates with the maximum power output thermoelectric materials can generate.[6,7]

The field of thermoelectrics is making steady progress; however, the current state-of-the-art commercial thermoelectric materials largely consist of inorganic materials with poor mechanical stability; are naturally scarce, toxic, cost intensive; and have high masses, such as PbTe, Bi_2Te_3, and Sb_2Te_3.[8,9] Current manufacturing techniques use spark plasma sintering (SPS) or hot pressuring, which requires high temperatures and pressures, resulting in long manufacturing times. The development of highly efficient alternatives to brittle inorganic thermoelectric materials is necessary to develop flexible TEGs, which could be more easily deployed than current rigid TEGs. Conducting polymers,[10−13] nanocarbons[14,15] and their composite materials[16,17] are widely researched owing to their low cost, lightweight, low thermal conductivity, mechanical flexibility, and easy processability.[18,19] Nanocarbon filler-based composites have shown impressive synergy of the constituent materials in terms of enhanced thermoelectric performance.[20,21] While, several recent reports show remarkable thermoelectric properties, they lack the fabrication of TEG modules and performance owing to their incompatibility with the required large-area fabrication techniques.[22] These studies, therefore, did not proceed beyond the characterization of the thermoelectric properties.[15,16,23] In

Received: December 22, 2020
Accepted: January 29, 2021
Published: February 10, 2021

https://dx.doi.org/10.1021/acsomega.0c06221
ACS Omega 2021, 6, 5019−5026

addition, organic-based thermoelectric materials or their composites generally demonstrate relatively low thermoelectric performance compared to their inorganic counterparts. This is due to their relatively low Seebeck coefficients and often low electrical conductivities.[24,25] In the context of the flexible thermoelectric materials, the performance has been significantly improved owing to the high electrical conductivity of organic polymers such as poly(3,4-ethylenedioxythiophene):poly(styrenesulfonate) (PEDOT:PSS). The sensitivity of conducting organic polymers due to the humidity in ambient conditions and the lack of stable n-type materials, however, leads to a limitation for practical applications of conducting polymers.[25,26] New cost-effective and lightweight materials that are paintable or printable, therefore, could be more useful and commercially viable even with relatively low thermoelectric performance. It is worth to note that two dimensional (2D) materials have been increasingly used in thermoelectric applications; a recent review on 2D thermoelectric materials was reported.[27]

To circumvent these issues, this work presents a unique, facile, extremely simple, and solvent-free low-cost method to develop thermoelectric devices. The resultant TEGs not only are flexible but also show promising low-temperature thermoelectric power output for a temperature gradient up to 70 K. However, if another substrate is used that can withstand more elevated temperatures, then the fabricated devices could be extended to higher-temperature applications. The devices originates from drawing on cheap and abundant ordinary office paper, which acts as an insulating substrate, while a slice of a compressed pellet bar of few-layered graphene (FLG) has been used as a p-type "pencil" to draw p-type only device and also the p-type leg of a p-n device. HB pencil traces were used to draw n-type legs. Graphene is the most widely studied instance of 2D materials for its applications in mechanical, electrical, and photonic industries owing to its unique properties;[28] however, it has limited thermoelectric potential due to its semi-metallic nature that ultimately results in low Seebeck coefficients.[29] Graphene also possess high κ that leads to the modest thermoelectric conversion efficiency.[30] Despite graphene-based polymer composites demonstrating promise in the low-temperature thermoelectrics,[22,31] only a few studies have focused on all graphene-based thermoelectrics.[32] Thus, graphene's potential in thermoelectrics is largely unexplored. The utilized FLG was sourced from a novel dry physical grinding technique followed by graphene nanoflakes liberation using plasma treatment and intercalation with dielectric barrier discharge (DBD) utilizing both atmospheric and vacuum process. Most importantly, our synthesized FLG possessed significantly lower κ[33] compared to other values reported for FLG,[34,35] which makes it suitable for thermoelectric applications. In addition, HB pencil traces comprise nanocomposites of graphite nanoparticles and multilayer sheets of graphene and clay.[36] Pencil drawn films, being electrically conductive and stable in different environments, have already been explored in several electronic devices such as supercapacitors,[37] photodiodes,[38] field effect transistors,[39] and photo-, tenzo-, and chemiresistive sensors.[40−42] Recently, Brus et al.[43] used HB pencil as an n-type material in a PEDOT:PSS based thermoelectric device. HB pencil traces potential as an n-type carbon-based material, and therefore, has been explored in this work to produce all carbon-based thermoelectric device dry-drawn on paper. This facile and solvent-free deposition approach and the nontoxic nature and abundance of employed materials open up possible applications in systems that operate at a low temperature range of operation such as its utilization on a human body and electronic equipment (e.g., mobiles and computers) mainboards, and possibly at higher temperatures with an alternative substrate.

2. EXPERIMENTAL SECTION

2.1. Materials. Regular office paper (90 g/m^2) and the HB graphite pencil (Wilko) were used as received. The p-type FLG was obtained from Perpetuus Carbon Technologies Ltd., UK. Silver conductive paint was purchased from RS components, UK.

2.2. Thin Films and Thermoelectric Characterizations. Paper was employed as the substrate for all the samples prepared during the current study. The p-type and n-type films were drawn on paper using a slice (pencil-like) of pressed pellet bar of FLG and an HB pencil lead traces, respectively, as shown in Figure 1b. The thicknesses of the paper-drawn n-type

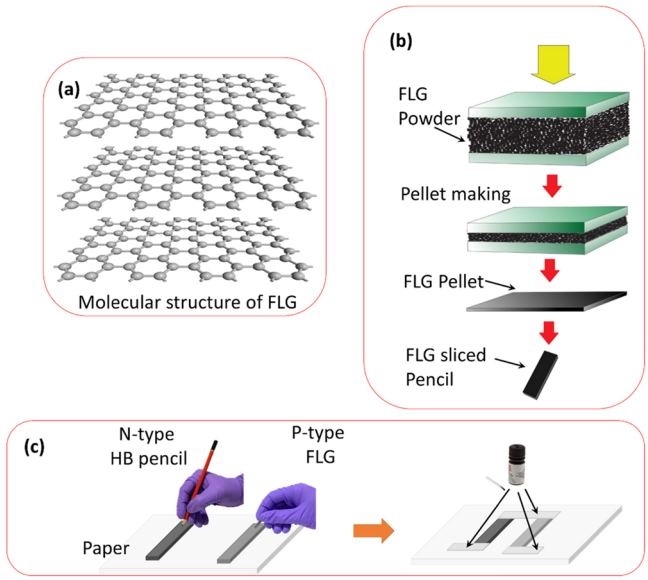

Figure 1. (a) Molecular structure of the FLG. Schematic of the (b) pellet making and (c) the device fabrication processes.

(HP graphite pencil) and p-type (FLG pellet bar) films were measured by surface profiler and determined to be ∼100 nm, with relative deviation of ±10%. Field emission scanning electron microscope (FESEM, Hitachi 4800 S, Japan) and a Renishaw inVia Qontor confocal Raman spectrometer with an excitation wavelength of 633 nm were used to examine the morphology and structural properties of the films, respectively. An optical phonon frequency (520.6 cm^{-1}) of single-crystal silicon was used to calibrate the Raman shifts. The reflecting microscope objective was 50×, n.a. 0.15, and the excitation spot diameter was 15 μm. The light was detected by a charge-coupled device and the samples were excited using a continuous-wave He-Ne laser emitting at 633 nm with a power of 500 mW. The Seebeck coefficient and the electrical properties of FLG and HB pencil trace drawn on paper were measured by fixing the paper onto a glass substrate for rigidity and using an ULVAC ZEM-3 with a helium atmosphere.

2.3. Device Fabrication. Onto the paper, the parallel legs measuring 3.0 cm × 0.5 cm each with an inter-legs separation

https://dx.doi.org/10.1021/acsomega.0c06221
ACS Omega 2021, 6, 5019−5026

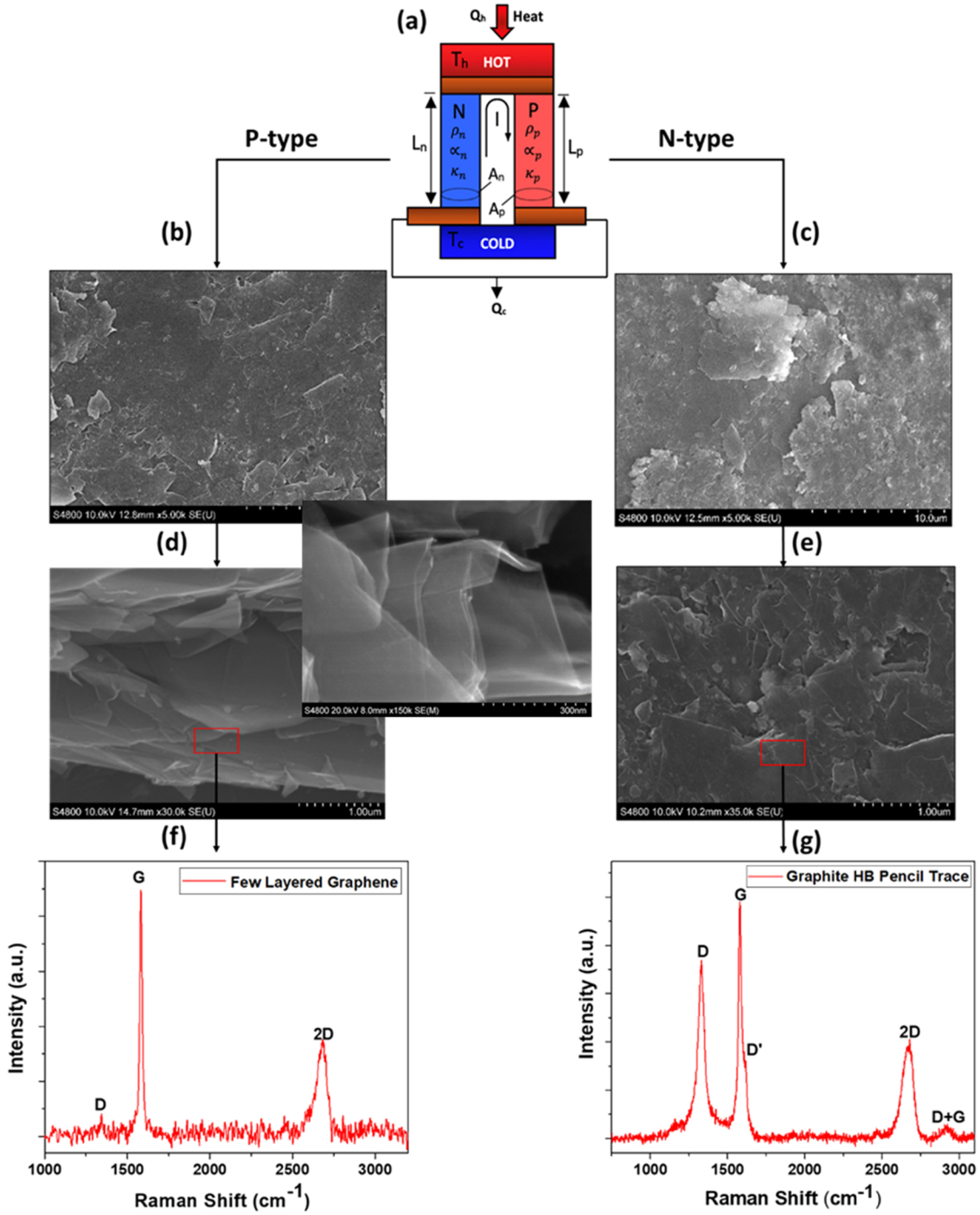

Figure 2. (a) Device architecture of the TEG unit; (b, c) low and (d, e) high magnification FESEM images of the morphology of FLG and pencil traces on paper, respectively. Inset shows the few-layered structure of the graphene. Raman spectra of (f) FLG and (g) pencil traces on paper.

of 0.5 cm were drawn using a pressed pellet bar of FLG to fabricate a p-type device only, whereas normal HB graphite pencil was used to draw n-type leg in the p-n device. Silver conductive paint was brush painted to make contacts.

2.4. Device Characterization. The open circuit voltage (V_{OC}) and the short-circuit current (I_{sc}) were measured using a Keithley 2401 digital multimeter. The hot side was heated using a digital hotplate model Elektrotechnik PR 53 T, while a custom-made passive cold stage has been designed to use as a heat sink to help maintain a temperature gradient. Two thermocouples, one on the cold side and the other on the hot side, were used to determine ΔT.

3. RESULTS AND DISCUSSION

3.1. Morphological and Structural Characterization of FLG and Pencil Traces. FESEM microscopy and Raman backscattering measurements were employed to evaluate the morphology and structural properties, respectively, of the FLG and pencil traces drawn on paper. The FLG images shown in Figure 2b,d exhibit large sized sheets of micrometer dimensions. The inset image taken from raw material shows

https://dx.doi.org/10.1021/acsomega.0c06221
ACS Omega 2021, 6, 5019−5026

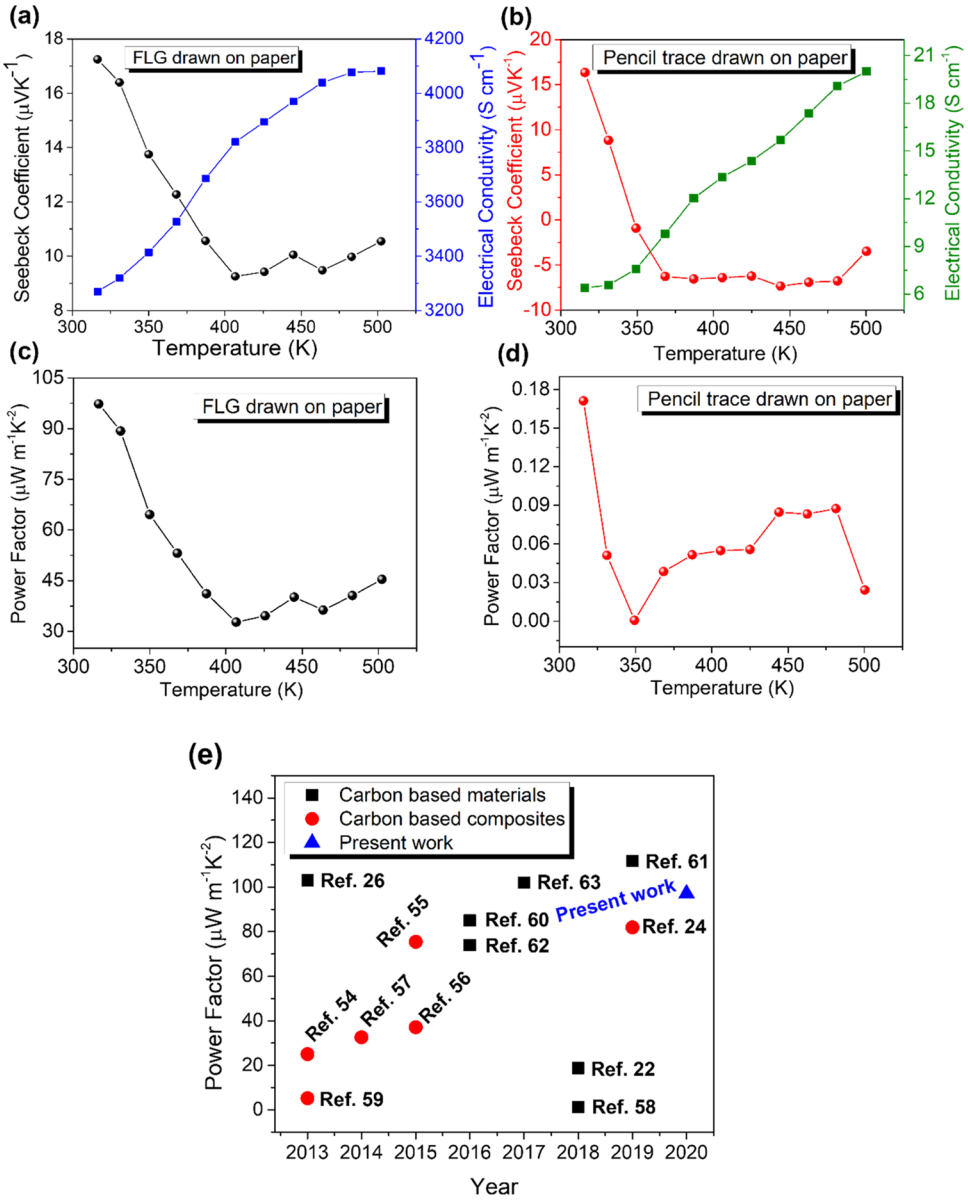

Figure 3. Thermoelectric characteristics of FLG and HB pencil drawn films on paper. Seebeck coefficient, electrical conductivity, and power factor of (a, c) FLG and (b, d) pencil trace, respectively. (e) Power factor values for the current work plus recently reported carbon-based TE materials and their composites.[22,24,26,54−63]

the few-layered structure of the graphene. It confirms the 2−3 graphene sheets stacked with each other with the space between the sheets visible. This suggests a high degree of exfoliation, which justifies that our prepared graphene is indeed nanoflakes of FLG. The nano-sized particles from FLG, however, probably penetrate into the paper to fill voids owing to the porous nature of paper. It is possible, therefore, that the films might partially repeat the morphology of the bare paper surface. The pencil traces on paper, in contrast, exhibit disordered stacks of graphite flakes with varied sizes (Figure 2c,e).

Raman spectra of FLG nanoflakes are depicted in Figure 2f. The main graphitic peak corresponding to the G band is at 1583 cm^{-1}, which represents the doubly degenerate phonon mode of sp^2 carbon.[44,45] The G band indicates the presence of graphene.[46] Apart from this, a less intense peak at 1347 cm^{-1} is ascribed to the D band, which constitutes defects in the sp^2 hybridized hexagonal sheet of graphene.[46] The 2D band is a second-order two-phonon process and is represented by a peak at 2683 cm^{-1}.[44] It is noteworthy that the intensity of D band and the intensity ratio of D and G bands (I_D/I_G) are directly proportional to the number of defects and number of layers in the graphene lattice, respectively.[47] Thus it can be interpreted that a low-intensity D band peak observed in our case represents very little or almost no defects in graphene lattice. In addition, the I_D/I_G ratio of 0.12 is much smaller than the previously reported data for FLG,[45,48] which also confirms the high quality and fewer number of layers of the FLG. Raman spectra of pencil traces on paper are depicted in Figure 2g, which shows peaks similar to those of polycrystalline graphite. The G band at 1580 cm^{-1} corresponds to the bond stretching of sp^2 hybridized atoms,[49] while the D and D′ bands at 1330 and 1617 cm^{-1} are ascribed to the disorder-induced mode from Raman scattering at the graphene edges.[37] The D peak also indicates the defects in the sp^2 graphite sheets. Moreover, as a common feature of polycrystalline graphite and the

https://dx.doi.org/10.1021/acsomega.0c06221
ACS Omega 2021, 6, 5019−5026

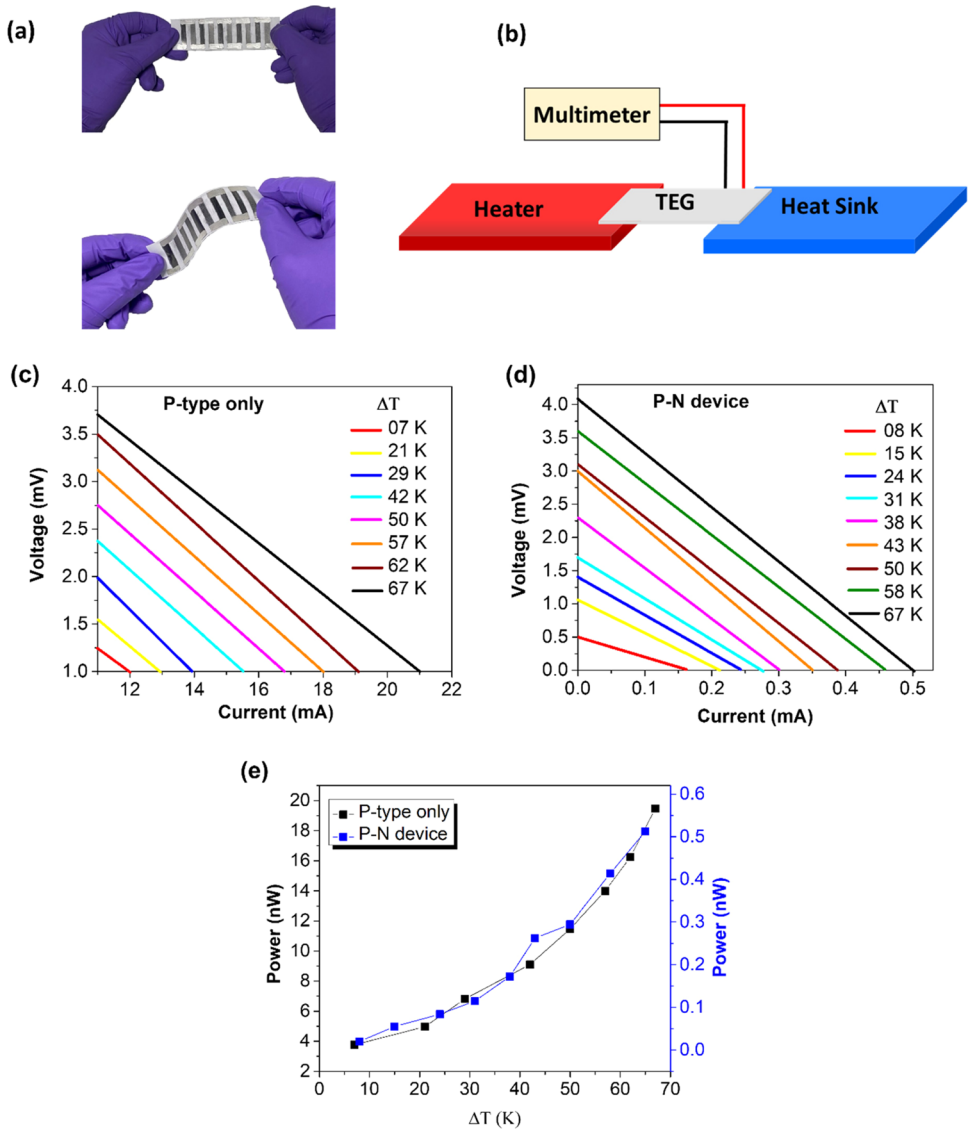

Figure 4. (a) A photograph of TE device drawn on paper using FLG and pencil traces. (b) Schematic of experimental setup to characterize the TEGs. Measured open circuit voltage (V_{oc}) and short-circuit current (I_{sc}) as a function of temperature gradient (ΔT) for the (c) P-type FLG only and (d) p-n device comprises of P-type FLG leg and N-type pencil trace leg drawn on paper. (e) Output power of the P-type only and P-N device drawn on paper assuming that $P_{max} = (V_{oc} \times I_{sc})/4$.[64,65]

graphite-like materials possessing crystalline defect, an overtone of D peak is denoted as a 2D peak has been observed at ~2681 cm^{-1}.[49,50] The D + G band appears at 2923 cm^{-1}. The presence of a strong D band could be due to two factors. First, fewer number of stacked graphene allows more edge planes to expose. Second, the degree of disorder in the deposited graphite increases owing to the shearing that induces less aligned AB stacking.[37,51]

3.2. Evaluation of Thermoelectric Characteristics. The thermoelectric characteristics of electrically conductivity and Seebeck coefficient were measured of the paper-drawn FLG and pencil traces. Due to the thin film nature of the samples, the thermal conductivity was not measured. The thermal conductivity of FLG pellets, however, has been seen to be 120 or 10 W m^{-1} K^{-1} at room temperature depending on the orientation of the FLG samples.[33] The Seebeck coefficient of FLG traces on paper exhibited p-type behavior and progressively decreased with increasing temperature from a maximum of 17 μV K^{-1} at 317 K to 9 μV K^{-1} at 407 K, as shown in Figure 3a, after which the Seebeck coefficient is seen to be almost stable despite a further increase in temperature. The electrical conductivity, however, is found to consistently increase with the increase in temperature. This follows an almost linear trend (Figure 3a), reaching a value of 4100 S cm^{-1} at 502 K. These electrical conductivity values are higher than those reported for FLG pellets,[33] showing (also defect-free graphene sheets are the reason for better electrical conductivity compared to previous reported ones) that the drawing method can enhance the electrical conductivity of FLG. This is most likely due to the rubbing action causing preferential alignment of FLG along the paper's plane. The initial inverse and direct correlation of Seebeck coefficient and electrical conductivity with temperature, respectively, can be explained due to elevation of physio-absorbed oxygen species from the FLG particles. This leads to an increase in carrier concentration, which results in higher electrical conductivity and lower Seebeck coefficients.[52] The resulting power factor of the FLG traces film on paper is presented in Figure 3c, which

https://dx.doi.org/10.1021/acsomega.0c06221
ACS Omega 2021, 6, 5019−5026

shows a similar trend to the Seebeck coefficient, due to the power factor being dependent on the square of the Seebeck coefficient. A maximum value of 97 μW m^{-1} K^{-2} at 317 K is seen, after which a sharp decrease is observed between 317 and 407 K, before stabilization. At more elevated temperatures, the power factor shows minimal variation with temperature. While these power factors are lower than that is typically seen for inorganic materials, they could be improved with the addition of highly conductive polymers such as PEDOT:PSS, where power factors with graphene of up to 2710 μW m^{-1} K^{-2} have been reported.[20] The Seebeck coefficient of pencil traces on paper is shown in Figure 3b. Initially, the pencil film is shown to act as a p-type material at lower temperatures between 316 and 331 K. The Seebeck coefficient progressively becomes negative; however, a majority of the carriers are switched from holes to electron as the temperature increases. We believe this could be occurring due to elevation of physio-absorbed oxygen species from the pencil trace particles, increasing the concentration of carrier electrons. It is possible, however, that the change from p- to n-type could be due to the introduction of oxygen functional groups.[53] The resulting Seebeck coefficient saturates at a value of −7 μV K^{-1} at 444 K. Recently, pencil trace on paper has been shown to be an n-type, where a Seebeck coefficient of −17.9 μV K^{-1} was measured using a home-made setup by linear fitting of experimentally measured ΔV at different ΔT values.[43] The measured Seebeck coefficient here, however, was made using a commercial ULVAC ZEM-3, which showed significantly lower values and initially p-type behavior. The lack of calibration for wire or other instrumental Seebeck coefficients in their study[43] could explain the difference in the values observed. Nonetheless, the results indicate that the pencil traces can exhibit weak n-type behavior when the temperature is elevated slightly above room temperature. It is possible, therefore, that pencil traces could be used as an n-type leg material in conjunction with the p-type FLG to form all carbon-based p-n thermoelectric devices. The electrical conductivity of the pencil traces linearly increased with increasing temperature, reaching to a maximum value of 20 S cm^{-1} at 500 K. This translates a maximum power factor of 0.17 μW m^{-1} K^{-2} at 316 K, which sharply decreased until 350 K, followed by a weak linear increase in the values. The FLG traces on paper showed a favorable power factor of 97 μW m^{-1} K^{-2}, when compared to recently reported only carbon TE materials produced in more complex synthesis techniques, and even compares favorably to some polymer composites. This is illustrated in Figure 3e.[22,24,26,54−63]

3.3. Paper-Drawn Thermoelectric Device Characterization. A photograph of the fabricated device and a schematic illustration of the testing setup are shown in Figure 4a and b, respectively. Figure 4c illustrates the V_{OC} and the I_{sc} of only p-type FLG based single TEG unit up to a ΔT of 67 K. Both the V_{OC} and the I_{sc} and the resulting calculated power output showed a linear increase with ΔT. At a ΔT of 67 K the TEG showed a voltage of 3.71 mV and a current of 21 μA, yielding a maximum output power of 19.48 nW (Figure 4e) assuming that $P_{max} = (V_{oc} \times I_{sc})/4$.[64,65] A p-n device was fabricated by employing pencil traces as the n-type leg. The p-n based TEG unit (containing two legs) showed lower performance with a maximum output power of 0.51 nW, with an I_{sc} of 0.5 μA and a V_{OC} of 4.1 mV at ΔT of 67 K (Figure 4d). While the voltage of the p-n device is slightly higher than that of the p-type only devices, due to the n-type nature of the pencil traces, the current is significantly lower. This is due to the low conductivity of the pencil traces compared to the FLG traces and due to the extra contact resistances formed from the extra junctions created to form the n-type legs. The resulting performance of the p-n device is, therefore, significantly lower than the p-type only device. Improving the low electrical conductivity of the HB pencil traces or fabricating compatible n-type FLG would significantly improve the performance of the p-n devices. Sheng et al.[61] reported SWCNTs with similar power factors to our FLG samples and successfully made well-matched p- and n-type samples, which resulted in a p-n device with a power output of up to 1.16 μW. The performance of the devices would also be significantly improved with the development of a fabrication processes that would enable thicker TE legs (current legs are ∼100 nm) to be realized. Were these improvements to be realized, then FLG trace TEGs could be used for self-powered sensor applications, such as temperature monitoring. Nevertheless, a power output 19.48 nW in the case of the p-type FLG based TEG and 0.51 nW for the p-n device is comparable to other only carbon TEGs reported in the literature. Nguyen et al.[66] reported an output power of 1.36 nW (24 p-n junctions) at ΔT of 50 K for the nitrogen-doped graphene derivatives and Rafiq et al.[67] demonstrated an output power of 1.75 nW (5 p-n junctions) at ΔT of 60 K for the graphite TEGs on paper.

4. CONCLUSIONS

In summary, we have demonstrated facile, cost-effective, large-area-compatible fabrication route for all only carbon-based films constituting FLG and HB pencil traces. Both the p-type and p-n-type devices were realized using the same fabrication process onto regular office paper. We demonstrate that FLG traces on paper showed promising thermoelectric parameters and device performance owing to the reasonably high thermoelectric parameters with the electrical conductivity and Seebeck coefficient of 41 S cm^{-1} and +17 μV K^{-1}, respectively, yielding a maximum power factor of 97 μW m^{-1} K^{-1} at 317 K. The pencil traces, however, showed poor thermoelectric parameters and device performance due to the weak n-type characteristics and higher resistance of the HB pencil compared to the FLG traces. The unexplored thermoelectric properties of FLG and pencil traces on a regular office paper as a substrate, however, constitute a potential approach for the development of flexible, extremely simple, ecologically and economically viable, solvent-free thermoelectric devices that can be used for low-temperature waste heat sources. Moreover, the current results demonstrated proof-of-concept TEGs drawn on paper.

AUTHOR INFORMATION

Corresponding Authors

Matthew R. Burton − *SPECIFIC, College of Engineering, Swansea University, Swansea SA1 8EN, United Kingdom*; Email: m.r.burton@swansea.ac.uk

Lijie Li − *College of Engineering, Swansea University, Swansea SA1 8EN, United Kingdom*; orcid.org/0000-0003-4630-7692; Email: l.li@swansea.ac.uk

Authors

Saqib Rafique − *College of Engineering, Swansea University, Swansea SA1 8EN, United Kingdom*

Nafiseh Badiei − *College of Engineering, Swansea University, Swansea SA1 8EN, United Kingdom*

https://dx.doi.org/10.1021/acsomega.0c06221
ACS Omega 2021, 6, 5019−5026

Jorge Eduardo Gonzalez-Feijoo − *College of Engineering, Swansea University, Swansea SA1 8EN, United Kingdom*
Matthew J. Carnie − *SPECIFIC, College of Engineering, Swansea University, Swansea SA1 8EN, United Kingdom;* orcid.org/0000-0002-4232-1967
Afshin Tarat − *Perpetuus Carbon Technologies Ltd., Swansea SA7 0AQ, United Kingdom*

Complete contact information is available at: https://pubs.acs.org/10.1021/acsomega.0c06221

Notes

The authors declare no competing financial interest.

■ ACKNOWLEDGMENTS

We would like to thank the Solar Photovoltaic Academic Research Consortium II (SPARC II) project, funded by WEFO for support. Moreover, the authors acknowledge the SPECIFIC Innovation and Knowledge Centre (EP/N020863/1) for funding. The authors would also like to thank COATED2 (EPSRC EP/L015099/1) for purchasing the ULVAC ZEM-3.

■ REFERENCES

(1) Forman, C.; Muritala, I. K.; Pardemann, R.; Meyer, B. Estimating the global waste heat potential. *Renew. and Sust. Energ. Rev.* **2016**, *57*, 1568−1579.
(2) Huewe, F.; Steeger, A.; Kostova, K.; Burroughs, L.; Bauer, I.; Strohriegl, P.; Dimitrov, V.; Woodward, S.; Pflaum, J. Low-Cost and Sustainable Organic Thermoelectrics Based on Low-Dimensional Molecular Metals. *Adv. Mater.* **2017**, *29*, No. 1605682.
(3) Ferhat, S.; Domain, C.; Vidal, J.; Noël, D.; Ratier, B.; Lucas, B. Organic thermoelectric devices based on a stable n-type nanocomposite printed on paper. *Sustainable Energy Fuels* **2018**, *2*, 199−208.
(4) Zebarjadi, M.; Esfarjani, K.; Dresselhaus, M.; Ren, Z.; Chen, G. Perspectives on thermoelectrics: from fundamentals to device applications. *Energy Environ. Sci.* **2012**, *5*, 5147−5162.
(5) Liu, W. D.; Chen, Z. G.; Zou, J. Eco-friendly higher manganese silicide thermoelectric materials: Progress and future challenges. *Adv. Energy Mater.* **2018**, *8*, No. 1800056.
(6) Moshwan, R.; Yang, L.; Zou, J.; Chen, Z. G. Eco-friendly SnTe thermoelectric materials: progress and future challenges. *Adv. Funct. Mater.* **2017**, *27*, No. 1703278.
(7) Hong, M.; Chen, Z. G.; Yang, L.; Liao, Z. M.; Zou, Y. C.; Chen, Y. H.; Matsumura, S.; Zou, J. Achieving zT> 2 in p-Type AgSbTe2−xSex Alloys via Exploring the Extra Light Valence Band and Introducing Dense Stacking Faults. *Adv. Energy Mater.* **2018**, *8*, No. 1702333.
(8) Biswas, K.; He, J.; Wang, G.; Lo, S.-H.; Uher, C.; Dravid, V. P.; Kanatzidis, M. G. High thermoelectric figure of merit in nanostructured p-type PbTe−MTe (M= Ca, Ba). *Energy Environ. Sci.* **2011**, *4*, 4675−4684.
(9) Kim, S. J.; We, J. H.; Cho, B. J. A wearable thermoelectric generator fabricated on a glass fabric. *Energy Environ. Sci.* **2014**, *7*, 1959−1965.
(10) Fan, Z.; Li, P.; Du, D.; Ouyang, J. Significantly Enhanced Thermoelectric Properties of PEDOT: PSS Films through Sequential Post-Treatments with Common Acids and Bases. *Adv. Energy Mater.* **2017**, *7*, No. 1602116.
(11) Zhang, Z.; Qiu, J.; Wang, S. Roll-to-roll printing of flexible thin-film organic thermoelectric devices. *Manufac. Lett.* **2016**, *8*, 6−10.
(12) Yao, H.; Fan, Z.; Cheng, H.; Guan, X.; Wang, C.; Sun, K.; Ouyang, J. Recent development of thermoelectric polymers and composites. *Macromol. Rapid Commun.* **2018**, *39*, No. 1700727.
(13) Bahk, J.-H.; Fang, H.; Yazawa, K.; Shakouri, A. Flexible thermoelectric materials and device optimization for wearable energy harvesting. *J. Mater. Chem. C* **2015**, *3*, 10362−10374.
(14) Avery, A. D.; Zhou, B. H.; Lee, J.; Lee, E.-S.; Miller, E. M.; Ihly, R.; Wesenberg, D.; Mistry, K. S.; Guillot, S. L.; Zink, B. L. Tailored semiconducting carbon nanotube networks with enhanced thermoelectric properties. *Nat. Energy* **2016**, *1*, 1−9.
(15) Kim, S. L.; Choi, K.; Tazebay, A.; Yu, C. Flexible power fabrics made of carbon nanotubes for harvesting thermoelectricity. *ACS Nano* **2014**, *8*, 2377−2386.
(16) Toshima, N.; Oshima, K.; Anno, H.; Nishinaka, T.; Ichikawa, S.; Iwata, A.; Shiraishi, Y. Novel hybrid organic thermoelectric materials: Three-component hybrid films consisting of a nanoparticle polymer complex, carbon nanotubes, and vinyl polymer. *Adv. Mater.* **2015**, *27*, 2246−2251.
(17) Mai, C.-K.; Russ, B.; Fronk, S. L.; Hu, N.; Chan-Park, M. B.; Urban, J. J.; Segalman, R. A.; Chabinyc, M. L.; Bazan, G. C. Varying the ionic functionalities of conjugated polyelectrolytes leads to both p- and n-type carbon nanotube composites for flexible thermoelectrics. *Energy Environ. Sci.* **2015**, *8*, 2341−2346.
(18) He, M.; Qiu, F.; Lin, Z. Towards high-performance polymer-based thermoelectric materials. *Energy Environ. Sci.* **2013**, *6*, 1352−1361.
(19) Chabinyc, M. Thermoelectric polymers: Behind organics' thermopower. *Nat. Mater.* **2014**, *13*, 119−121.
(20) Cho, C.; Wallace, K. L.; Tzeng, P.; Hsu, J. H.; Yu, C.; Grunlan, J. C. Outstanding low temperature thermoelectric power factor from completely organic thin films enabled by multidimensional conjugated nanomaterials. *Adv. Energy Mater.* **2016**, *6*, No. 1502168.
(21) (a) Cho, C.; Wallace, K.; Tzeng, P.; Hsu, J.; Yu, C. Outstanding Low Temperature Thermoelectric Power Factor from Completely Organic Thin Films Enabled by Multidimensional Conjugated Nanomaterials. *Adv. Energy Mater.* **2016**, *6*, 1−8. (b) Cho, C.; Stevens, B.; Hsu, J.-H.; Bureau, R.; Hagen, D. A.; Regev, O.; Yu, C.; Grunlan, J. C. Completely organic multilayer thin film with thermoelectric power factor rivaling inorganic tellurides. *Adv. Mater.* **2015**, *27*, 2996−3001.
(22) Juntunen, T.; Jussila, H.; Ruoho, M.; Liu, S.; Hu, G.; Albrow-Owen, T.; Ng, L. W.; Howe, R. C.; Hasan, T.; Sun, Z. Inkjet printed large-area flexible few-layer graphene thermoelectrics. *Adv. Funct. Mater.* **2018**, *28*, No. 1800480.
(23) Zhou, W.; Fan, Q.; Zhang, Q.; Li, K.; Cai, L.; Gu, X.; Yang, F.; Zhang, N.; Xiao, Z.; Chen, H. Ultrahigh-power-factor carbon nanotubes and an ingenious strategy for thermoelectric performance evaluation. *Small* **2016**, *12*, 3407−3414.
(24) Hsieh, Y.-Y.; Zhang, Y.; Zhang, L.; Fang, Y.; Kanakaraaj, S. N.; Bahk, J.-H.; Shanov, V. High thermoelectric power-factor composites based on flexible three-dimensional graphene and polyaniline. *Nanoscale* **2019**, *11*, 6552−6560.
(25) Cho, C.; Bittner, N.; Choi, W.; Hsu, J. H.; Yu, C.; Grunlan, J. C. Thermally Enhanced n-Type Thermoelectric Behavior in Completely Organic Graphene Oxide-Based Thin Films. *Adv. Electr. Mater.* **2019**, *5*, No. 1800465.
(26) Park, K. T.; Choi, J.; Lee, B.; Ko, Y.; Jo, K.; Lee, Y. M.; Lim, J. A.; Park, C. R.; Kim, H. High-performance thermoelectric bracelet based on carbon nanotube ink printed directly onto a flexible cable. *J. Mater. Chem. A* **2018**, *6*, 19727−19734.
(27) Li, D.; Gong, Y.; Chen, Y.; Lin, J.; Khan, Q.; Zhang, Y.; Li, Y.; Zhang, H.; Xie, H. Recent Progress of Two-Dimensional Thermoelectric Materials. *Nano-Micro Lett.* **2020**, *12*, 36.
(28) Bonaccorso, F.; Sun, Z.; Hasan, T.; Ferrari, A. Graphene photonics and optoelectronics. *Nat. Photonics* **2010**, *4*, 611.
(29) Dollfus, P.; Nguyen, V. H.; Saint-Martin, J. Thermoelectric effects in graphene nanostructures. *J. Phys.: Condens. Matter* **2015**, *27*, No. 133204.
(30) Pop, E.; Varshney, V.; Roy, A. K. Thermal properties of graphene: Fundamentals and applications. *MRS Bull.* **2012**, *37*, 1273−1281.

(31) Chen, G.; Xu, W.; Zhu, D. Recent advances in organic polymer thermoelectric composites. *J. Mater. Chem. C* **2017**, *5*, 4350−4360.
(32) Guo, Y.; Mu, J.; Hou, C.; Wang, H.; Zhang, Q.; Li, Y. Flexible and thermostable thermoelectric devices based on large-area and porous all-graphene films. *Carbon* **2016**, *107*, 146−153.
(33) Rafique, S.; Burton, M. R.; Badiei, N.; Gonzalez-Feijoo, J. E.; Mehraban, S.; Carnie, M.; Tarat, A.; Li, L. Lightweight and Bulk Organic Thermoelectric Generators Employing Novel P-type Few Layered Graphene Nano-flakes. *ACS Appl. Mater. Interfaces* **2020**, *12*, 30643.
(34) Ghosh, S.; Bao, W.; Nika, D. L.; Subrina, S.; Pokatilov, E. P.; Lau, C. N.; Balandin, A. A. Dimensional crossover of thermal transport in few-layer graphene. *Nat. Mater.* **2010**, *9*, 555−558.
(35) Jeong, J.; Lee, K.; Shrestha, R.; Horne, K.; Das, S.; Choi, W.; Kim, M.; Choi, T. Thermal conductivity measurement of few layer graphene film by a micropipette sensor with laser point heating source. *Mater. Res. Exp.* **2016**, *3*, No. 055004.
(36) Wang, Y.; Zhou, H. To draw an air electrode of a Li−air battery by pencil. *Energy Environ. Sci.* **2011**, *4*, 1704−1707.
(37) Zheng, G.; Hu, L.; Wu, H.; Xie, X.; Cui, Y. Paper supercapacitors by a solvent-free drawing method. *Energy Environ. Sci.* **2011**, *4*, 3368−3373.
(38) Brus, V.; Maryanchuk, P. Graphite traces on water surface−A step toward low-cost pencil-on-semiconductor electronics and optoelectronics. *Carbon* **2014**, *78*, 613−616.
(39) Kurra, N.; Kulkarni, G. U. Pencil-on-paper: electronic devices. *Lab Chip* **2013**, *13*, 2866−2873.
(40) Brus, V.; Maryanchuk, P.; Kovalyuk, Z.; Abashyn, S. 2D nanocomposite photoconductive sensors fully dry drawn on regular paper. *Nanotechnology* **2015**, *26*, No. 255501.
(41) Lin, C.-W.; Zhao, Z.; Kim, J.; Huang, J. Pencil drawn strain gauges and chemiresistors on paper. *Sci. Rep.* **2014**, *4*, 3812.
(42) Smith, M. K.; Jensen, K. E.; Pivak, P. A.; Mirica, K. A. Direct self-assembly of conductive nanorods of metal−organic frameworks into chemiresistive devices on shrinkable polymer films. *Chem. Mater.* **2016**, *28*, 5264−5268.
(43) Brus, V. V.; Gluba, M.; Rappich, J. r.; Lang, F.; Maryanchuk, P. D.; Nickel, N. H. Fine art of thermoelectricity. *ACS Appl. Mater. Interfaces* **2018**, *10*, 4737−4742.
(44) Ferrari, A. C.; Meyer, J.; Scardaci, V.; Casiraghi, C.; Lazzeri, M.; Mauri, F.; Piscanec, S.; Jiang, D.; Novoselov, K.; Roth, S. Raman spectrum of graphene and graphene layers. *Phys. Rev. Lett.* **2006**, *97*, No. 187401.
(45) Rao, K. S.; Senthilnathan, J.; Liu, Y.-F.; Yoshimura, M. Role of peroxide ions in formation of graphene nanosheets by electrochemical exfoliation of graphite. *Sci. Rep.* **2014**, *4*, 1−6.
(46) Peng, K.-J.; Wu, C.-L.; Lin, Y.-H.; Liu, Y.-J.; Tsai, D.-P.; Pai, Y.-H.; Lin, G.-R. Hydrogen-free PECVD growth of few-layer graphene on an ultra-thin nickel film at the threshold dissolution temperature. *J. Mater. Chem. C* **2013**, *1*, 3862−3870.
(47) Gautam, M.; Shi, Z.; Jayatissa, A. H. Graphene films as transparent electrodes for photovoltaic devices based on cadmium sulfide thin films. *Sol. Energy Mater. Sol. Cells* **2017**, *163*, 1−8.
(48) Lin, P.-C.; Wu, J.-Y.; Liu, W.-R. Green and facile synthesis of few-layer graphene via liquid exfoliation process for Lithium-ion batteries. *Sci. Rep.* **2018**, *8*, 1−8.
(49) Knápek, A.; Sobola, D.; Burda, D.; Daňhel, A.; Mousa, M.; Kolařík, V. Polymer Graphite Pencil Lead as a Cheap Alternative for Classic Conductive SPM Probes. *Nanomaterials* **2019**, *9*, 1756.
(50) Tekenya, R.; Pokpas, K.; Jahed, N.; Iwuoha, E. I. Enhanced specificity and sensitivity for the determination of nickel (II) by square-wave adsorptive cathodic stripping voltammetry at disposable graphene-modified pencil graphite electrodes. *Anal. Lett.* **2019**, *52*, 373−398.
(51) Pimenta, M.; Dresselhaus, G.; Dresselhaus, M. S.; Cancado, L.; Jorio, A.; Saito, R. Studying disorder in graphite-based systems by Raman spectroscopy. *Phys. Chem. Chem. Phys.* **2007**, *9*, 1276−1290.
(52) Snyder, G. J.; Toberer, E. S. Complex thermoelectric materials. *Nat. Mater.* **2008**, *7*, 105−114.
(53) Tu, N. D. K.; Choi, J.; Park, C. R.; Kim, H. Remarkable Conversion Between n- and p-Type Reduced Graphene Oxide on Varying the Thermal Annealing Temperature. *Chem. Mater.* **2015**, *27*, 7362−7369.
(54) Nonoguchi, Y.; Ohashi, K.; Kanazawa, R.; Ashiba, K.; Hata, K.; Nakagawa, T.; Adachi, C.; Tanase, T.; Kawai, T. Systematic conversion of single walled carbon nanotubes into n-type thermoelectric materials by molecular dopants. *Sci. Rep.* **2013**, *3*, 1−7.
(55) Fukumaru, T.; Fujigaya, T.; Nakashima, N. Development of n-type cobaltocene-encapsulated carbon nanotubes with remarkable thermoelectric property. *Sci. Rep.* **2015**, *5*, 7951.
(56) Yoo, D.; Kim, J.; Lee, S. H.; Cho, W.; Choi, H. H.; Kim, F. S.; Kim, J. H. Effects of one-and two-dimensional carbon hybridization of PEDOT: PSS on the power factor of polymer thermoelectric energy conversion devices. *J. Mater. Chem. A* **2015**, *3*, 6526−6533.
(57) Li, F.; Cai, K.; Shen, S.; Chen, S. Preparation and thermoelectric properties of reduced graphene oxide/PEDOT: PSS composite films. *Synth. Met.* **2014**, *197*, 58−61.
(58) Okhay, O.; Gonçalves, G.; Dias, C.; Ventura, J.; Vieira, E.; Gonçalves, L.; Tkach, A. Tuning electrical and thermoelectric properties of freestanding graphene oxide papers by carbon nanotubes and heat treatment. *J. Alloys Compd.* **2019**, *781*, 196−200.
(59) Xu, K.; Chen, G.; Qiu, D. Convenient construction of poly (3, 4-ethylenedioxythiophene)−graphene pie-like structure with enhanced thermoelectric performance. *J. Mater. Chem. A* **2013**, *1*, 12395−12399.
(60) Hayashi, D.; Nakai, Y.; Kyakuno, H.; Yamamoto, T.; Miyata, Y.; Yanagi, K.; Maniwa, Y. Improvement of thermoelectric performance of single-wall carbon nanotubes by heavy doping: effect of one-dimensional band multiplicity. *Appl. Phys. Express* **2016**, *9*, No. 125103.
(61) Sheng, M.; Wang, Y.; Liu, C.; Xiao, Y.; Zhu, P.; Deng, Y. Significantly enhanced thermoelectric performance in SWCNT films via carrier tuning for high power generation. *Carbon* **2020**, *158*, 802−807.
(62) Nonoguchi, Y.; Iihara, Y.; Ohashi, K.; Murayama, T.; Kawai, T. Air-tolerant Fabrication and Enhanced Thermoelectric Performance of n-Type Single-walled Carbon Nanotubes Encapsulating 1, 1′-Bis (diphenylphosphino) ferrocene. *Chem.−An Asian J.* **2016**, *11*, 2423−2427.
(63) Nonoguchi, Y.; Sudo, S.; Tani, A.; Murayama, T.; Nishiyama, Y.; Uda, R. M.; Kawai, T. Solvent basicity promotes the hydride-mediated electron transfer doping of carbon nanotubes. *Chem. Commun.* **2017**, *53*, 10259−10262.
(64) Fan, P.; Zheng, Z.-H.; Li, Y.-Z.; Lin, Q.-Y.; Luo, J.-T.; Liang, G.-X.; Cai, X.-M.; Zhang, D.-P.; Ye, F. Low-cost flexible thin film thermoelectric generator on zinc based thermoelectric materials. *Appl. Phys. Lett.* **2015**, *106*, No. 073901.
(65) Burton, M. R.; Liu, T.; McGettrick, J.; Mehraban, S.; Baker, J.; Pockett, A.; Watson, T.; Fenwick, O.; Carnie, M. J. Thin film tin selenide (SnSe) thermoelectric generators exhibiting ultralow thermal conductivity. *Adv. Mater.* **2018**, *30*, No. 1801357.
(66) Tu, N. D. K.; Lim, J. A.; Kim, H. A mechanistic study on the carrier properties of nitrogen-doped graphene derivatives using thermoelectric effect. *Carbon* **2017**, *117*, 447−453.
(67) Mulla, R.; Jones, D. R.; Dunnill, C. W. Thermoelectric Paper: Graphite Pencil Traces on Paper to Fabricate a Thermoelectric Generator. *Adv. Mater. Technol.* **2020**, No. 2000227.

https://dx.doi.org/10.1021/acsomega.0c06221
ACS Omega 2021, 6, 5019−5026